DEVELOPMENT OF A FLAT FREQUENCY RESPONSE PRESSURE TRANSDUCER SYSTEM

BY

John Michael Lewis

United States
Naval Postgraduate School



THESIS

DEVELOPMENT OF A FLAT FREQUENCY

RESPONSE PRESSURE TRANSDUCER SYSTEM

by

John Michael Lewis II

June 1970

This document has been approved for public release and sale; its distribution is unlimited.

T136102

Development of a Flat Frequency Response Pressure Transducer System

by

John Michael Lewis II
Lieutenant (jg), United States Navy
B.S.A.E., United States Naval Academy, 1969

Submitted in partial fulfillment of the
requirements for the degree of

MASTER OF SCIENCE IN AERONAUTICAL ENGINEERING

from the

NAVAL POSTGRADUATE SCHOOL
June 1970

LIBRARY
NAVAL POSTGRADUATE SCHOOL
MONTEREY, CALIF. 93940

ABSTRACT

A theoretical prediction to determine the frequency response of a cascaded remote pressure transducer system has been developed. This prediction was used to find a theoretical configuration which would produce a fairly flat frequency response (1.00 ± 0.05) over a 100 hertz range. Such a configuration would allow cross-correlation of an unsteady, random, low-speed flow field by simple analog methods.

The theoretical prediction did not hold true for configurations of three serially connected tubes, but the parameters, namely, transducer volume, tube length, and tube diameter, proved the same trends experimentally that were predicted theoretically. By observing these trends, a solution of 1.00 ± 0.09 over a 95 hertz range was obtained.

TABLE OF CONTENTS

I. INTRODUCTION ---------- 11

II. EXPERIMENTAL PROCEDURE ---------- 12

A. GENERAL ---------- 12

B. THEORETICAL BACKGROUND ---------- 12

C. COMPUTER TECHNIQUE ---------- 15

D. EQUIPMENT ---------- 16

1. Pressure Transducers ---------- 16

2. Calibration Chamber ---------- 16

E. CALIBRATION ---------- 17

1. General ---------- 17

2. Proximeter Calibration ---------- 17

3. Static Calibration ---------- 18

4. Dynamic Calibration ---------- 18

F. EXPERIMENTATION ---------- 21

III. DISCUSSION AND RESULTS ---------- 24

IV. CONCLUSIONS AND RECOMMENDATIONS ---------- 40

APPENDIX A THEORETICAL RESPONSE OF A REMOTELY LOCATED PRESSURE TRANSDUCER SYSTEM ------ 42

APPENDIX B COMPUTERIZATION OF THE THEORETICAL RESPONSE OF A REMOTE PRESSURE TRANSDUCER SYSTEM ---------- 49

APPENDIX C CROSS-CORRELATION OF A RANDOM UNSTEADY SIGNAL ---------- 52

LIST OF REFERENCES ---------- 56

INITIAL DISTRIBUTION LIST ---------- 57

FORM DD 1473 ---------- 59

LIST OF FIGURES

FIGURE		PAGE
1.	SINGLE AND CASCADED PRESSURE TRANSDUCER SYSTEM ----------	13
2.	STATIC CALIBRATION INSTRUMENTATION ----------	19
3.	STATIC CALIBRATION CURVE ----------	20
4.	DYNAMIC CALIBRATION INSTRUMENTATION ----------	22
5.	SINGLE TUBE CONFIGURATION RESULTS ----------	25
6.	DESIRED THEORETICAL 2 AND 3 TUBE CONFIGURATION FREQUENCY RESPONSES ----------	26
7.	TWO TUBE CONFIGURATION RESULTS ----------	27
8.	(a) DESIRED THREE TUBE CONFIGURATION --------	29
	(b), (c) THREE TUBE CONFIGURATION RESULTS --------	30/31
	(d) MOST USEABLE THREE TUBE CONFIGURATION ---	32
9.	THEORETICAL TRENDS ----------	33
10.	EXPERIMENTAL TRENDS ----------	34
11.	CROSS-CORRELATION CIRCUIT ----------	36
12.	COMPUTER PROGRAM FLOWCHART	51

TABLE OF SYMBOLS

Latin Symbols

a_o	Mean velocity of sound
d	Tube inside diameter
D	Characteristic length of model
f	Frequency, hertz
g	Gravity constant
i	Imaginary unit = $\sqrt{-1}$
J_n	Bessel function of first kind of order n
K	Polytropic gas constant
L	Tube length
$\overline{p}$	Total value of static pressure
p_o	Mean value of static pressure
p	Amplitude of pressure disturbance
p_{o1}	Stagnation pressure
$p_1(t)$	Chamber pressure
$\hat{p}_1(t)$	Pressure transmitted through tube
Pr	Prandtl number
r	Radial coordinate
R	Tube radius
R_{12}	Cross-correlation coefficient for stations (1) and (2)
$\overline{R}$	Universal gas constant

S Strouhal number $= \frac{fD}{U}$

$\overline{T}$ Total temperature inside tube

T_o Mean temperature inside tube

t Time

T Amplitude of temperature disturbance inside tube

U Free stream velocity

$\overline{u}$ Complex velocity component in axial direction inside tube

u Amplitude of $\overline{u}$

$\overline{v}$ Complex velocity component in radial direction inside tube

v Amplitude of $\overline{v}$

V_v Volume of pressure transducer

V_t Tube volume

Greek Symbols

α Wave number

γ Ratio of specific

Θ Phase angle

λ Coefficient of thermal conductivity

μ Absolute fluid viscosity

ω Circular frequency, radians per second

$\bar{\rho}$ Fluid density

ρ_o Mean fluid density

ρ Amplitude of fluid density disturbance

τ Time constant

ACKNOWLEDGEMENTS

The author wishes to express his gratitude to Dr. Louis V. Schmidt, Department of Aeronautics, for his guidance and support as thesis advisor during the included work, and in particular for his design of the pressure transducers and his advice on their calibration.

The author also wishes to express appreciation to electronics technician Cecil Gordon for his advice and construction of the necessary circuits and instrumentation.

I. INTRODUCTION

Because of the increasing interest in measuring oscillatory and random unsteady flow fields on lightweight aeroelastic models, a need has gradually developed over the past several years for a direct measuring remote pressure transducer system to allow rapid and economical determination of auto- and cross-correlation type information plus the attendant spectral distribution. Such a system has been developed by Bergh [1] at the National Aeronautical and Astronautical Research Institute (N.L.R.) in Amsterdam, Holland, utilizing precise lengths of tubing to connect the remote pressure transducers with static orifices located on the model surfaces. Johnson [2] has confirmed Bergh's one tube theory and Allen [3] utilized a two tube configuration: both of these systems required compensation for the system's transfer function to be included in the data reduction process.

Should a configuration be found which would produce a flat frequency response over a specified range, cross-correlation of an unsteady, random signal could be achieved directly through the use of an analog circuit. Since a direct analog process does not readily allow for correction of the system's transfer function, the primary purpose of the subject program was to attain a useable flat frequency response of 1.0 ± 0.05 over a 0 - 100 hertz frequency range. This would allow direct evaluation of the unsteady aerodynamics in many low-speed flow fields of interest.

II. EXPERIMENTAL PROCEDURE

A. GENERAL

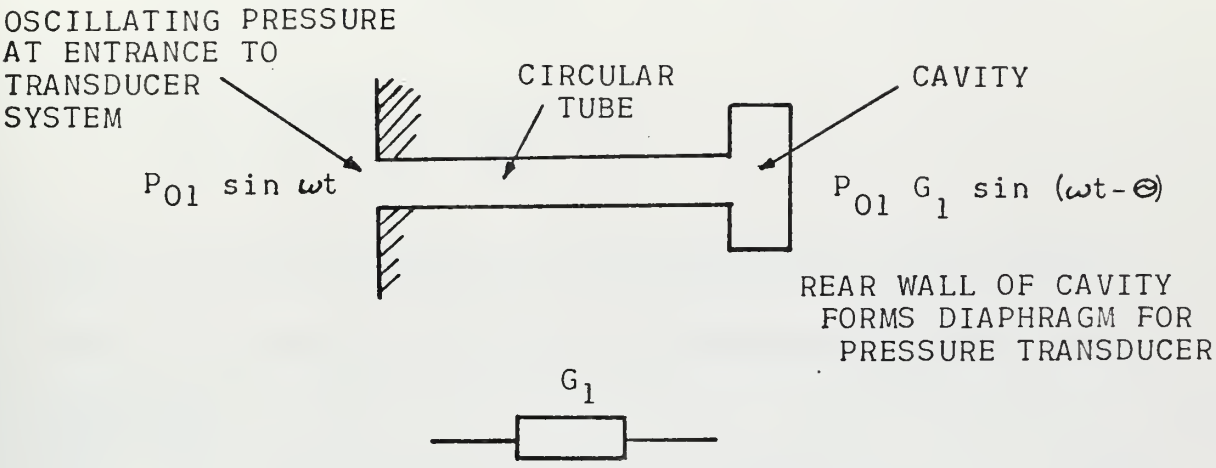
All experimentation was performed either in the Aero-Mechanics Laboratory, Room 022, Halligan Hall, or with the IBM 360-67 digital computer available at the U. S. Naval Postgraduate School.

B. THEORETICAL BACKGROUND

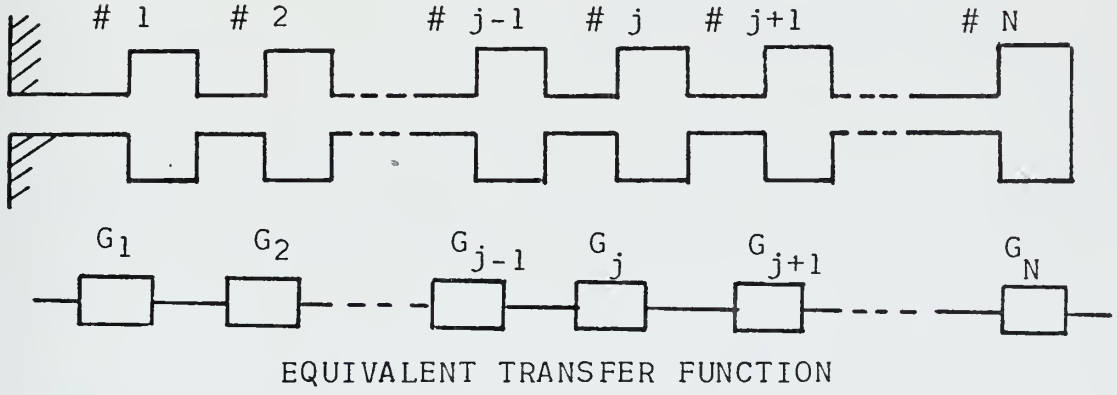
Bergh [1] has developed a theoretical prediction for the pressure ratio of not only a single tube remote pressure transducer system (Figure 1a) but also for a cascaded tube system employing N tubes such as shown in Figure 1b. The solution is based on several assumptions; the perturbations are of a sinusoidal nature imposed on the average values of the parameters, fluid flow in the tubes is assumed laminar, and the tube lengths are much larger than their diameters. By introducing these assumptions, the governing equations, i.e., the Navier-Stokes, continuity, energy, and state equations are reduced to a set of partial differential equations which may be solved subject to satisfying the boundary conditions. The mass flow rates of the air in the system between any two adjacent tubes must be equivalent. This relation provides an equation which reduces to the following form:

$$\frac{P_j}{P_{j-1}} = \left[\cosh\left(\phi_j L_j\right) + \frac{\omega^2}{a_o^2} \frac{\gamma}{K} \frac{V_{v_j}}{V_{t_j}} \frac{L_j}{\phi_j} \frac{J_0(\alpha_j)}{J_2(\alpha_j)} \sinh\left(\phi_j L_j\right) \right. \tag{1}$$

$$\left. + \frac{V_{t_{j+1}}}{V_{t_j}} \frac{L_j}{L_{j+1}} \frac{\phi_{j+1}}{\phi_j} \frac{J_2(\alpha_{j+1})}{J_0(\alpha_{j+1})} \frac{\sinh\left(\phi_j L_j\right)}{\sinh\left(\phi_{j+1} L_{j+1}\right)} \left\{ \cosh\left(\phi_{j+1} L_{j+1}\right) - \frac{P_{j+1}}{P_j} \right\} \right]$$



(a) SINGLE COMPONENT PRESSURE TRANSDUCER SYSTEM



(b) MULTIPLE COMPONENT PRESSURE TRANSDUCER SYSTEM

FIGURE 1

SINGLE AND CASCADED PRESSURE
TRANSDUCER SYSTEM

where:

$$\phi_j = \frac{\omega}{a_o} \gamma^{1/2} \left\{ \frac{J_o(\alpha_j)}{J_2(\alpha_j)} \right\}^{1/2} \left[1 + \frac{\gamma - 1}{\gamma} \frac{J_2(\alpha_j P_r^{1/2})}{J_o(\alpha_j P_r^{1/2})} \right]^{1/2}$$

$$\alpha_j = i^{3/2} R_j \left(\frac{\rho_o \omega}{\mu} \right)^{1/2}$$

When a single tube configuration (see Figure 1a) is used, the entire third term of equation (1) disappears, simplifying the equation to the form below:

$$\frac{P_j}{P_{j-1}} = \left[\cosh(\phi_j L_j) + \frac{\omega^2}{a_o^2} \frac{\gamma}{K} \frac{V_{v_j}}{V_{t_j}} \frac{L_j}{\phi_j} \frac{J_o(\alpha_j)}{J_2(\alpha_j)} \sinh(\phi_j L_j) \right]^{-1} \quad (2)$$

The subscript j refers to the tubes being analyzed in the N tube system. From equation (1) it is seen that the pressure ratio prediction is a function of tubes j-1 and j+1 as well as tube j, which in turn presents difficulties when optimizing the problem for the desired result. The solution complexity is not obvious at first; however, a closer inspection bears out that all the Bessel functions are functions of the imaginary parameter, $i^{3/2}$ which are sometimes called Kelvin functions [4] and hence, the solution is a complex quantity. The complex pressure ratio specifies not only the pressure ratio magnitude but also the phase shift. The equation also contains two uncertain quantities; the increase in transducer volume due to diaphragm deflection, and the polytropic gas constant, k. Bergh proved both of these terms to have only minor effects on the solutions to equations (1) and (2) and hence adiabatic flow was assumed while transducer volume changes were ignored. The system

can be represented by the acoustic analogy provided by Olson [5] for a multi-degree of freedom system. The analogy develops equations of motion for a sound wave of pressure p travelling in a tube and impinging on a cavity volume, with the resistance represented by the viscosity and the capacitance term dependent on the cavity volume. Similarly, Bergh's solution predicts the complex pressure ratio with the resistance and capacitance again represented by fluid viscosity and cavity volume, respectively.

C. COMPUTER TECHNIQUE

With the aid of Bergh's equations, the pressure ratio at a certain frequency can now be predicted. However, because the pressure ratio of the next higher tube is part of the predicted ratio and the tube size and cavity volume interact in an irregular manner, the total solution does not lend itself for routine optimizing techniques to produce a flat frequency response. Therefore the equations were programmed for a digital computer to facilitate pressure response prediction using program-operator chosen configurations. The program was designed for use on the IBM timesharing system but can also be used for batch processing, and contained a program option allowing the selection of either a one-, two-, or three-tube configuration. Each tube stage in a multiple tube configuration is specified by three parameters: transducer volume, tube length, and tube diameter. The program was verified for proper operation by comparing it with both a hand-worked calculation

for a one-tube configuration and Bergh's [1] results for both one- and two-tube configurations.

D. EQUIPMENT

1. Pressure Transducers

The two pressure transducers were designed by Professor L. V. Schmidt [6], and consisted of a Bentley Detector System mounted behind a 0.003-inch thick annealed brass diaphragm which was inserted in an aluminum housing. The diaphragm thickness was selected to give optimum sensitivity in a $\pm$ 0.75 psi range. The detector system consisted of a Bentley 316 AJW proximity detector inserted into a brass diaphragm holder. The proximity detector was a reluctance gage which sensed change in the air gap between the reluctance coil and a metal target, in this case the brass diaphragm. The diaphragm deflection was directly proportional to an applied pressure perturbation, and the proximity detector output was linear with respect to the diaphragm deflection; therefore, the output was a relative measurement of the pressure applied to the diaphragm.

2. Calibration Chamber

The calibration chamber was the same as used by Johnson [2] and consisted of an aluminum block with a 1.5-inch diameter cylindrical chamber 6 inches long. The chamber ends were designed to accept either the transducer holders or the adapter plates which connected the chamber to a remote transducer through the transmitting tubes. The chamber had a pressure port to allow the mean static pressure to be

varied from an external source, and also a threaded orifice designed to accept either a solid plug or a University Sound ID-75 acoustical driver unit. Both orifices were located at the chamber's midpoint so that unsteady pulses were introduced symmetrically to both transducer systems, namely the reference transducer at one end and the complete transducer system at the other end.

E. CALIBRATION

1. General

All calibration procedures were identical to those performed by Johnson [2] and Allen [3].

2. Proximeter Calibration

The Bentley 316 AJW proximity detectors were usually calibrated in order to determine the voltage output with respect to the air gap between the reluctance coil face and a metal target. By mounting a metal target on a micrometer stem, the target could be backed off known distances from the reluctance coil and the output monitored on a D.C. voltmeter. The Bentley D252 carrier amplifiers have a variable amplification capability which may be adjusted until the proximity detector output varies proportionately with the target distance. Because of the large apparent sensitivity of the proximity detectors, this procedure was foregone and the detectors were calibrated with respect to the pressure differential across the diaphragm during the static calibration procedures. The proximity detectors were inserted into the brass

diaphragm holders until their output was -3.0 volts D.C.: this was the range where transducer output and diaphragm deflection varied linearly.

3. Static Calibration

The transducer output was connected to a Bentley D252 carrier amplifier powered by a -18.0 volt D.C. regulated power supply. By inputing the carrier amplifier output simultaneously with a biasing voltage into an Astro-Data D885 differential amplifier, the differential amplifier output, monitored on a D.C. digital voltmeter, was adjusted to read zero for zero pressure differential across the diaphragm. A U-tube manometer and hand crank pump conveniently allowed known pressure differentials to be introduced into the calibration chamber for static sensitivity determination. The complete instrumentation diagram is shown in Figure 2. Each proximity detector was calibrated during this stage by introducing positive and negative pressure differentials of equal magnitudes into the calibration chamber and adjusting each carrier amplifier until the output was approximately the same for equal but opposite pressure differentials over a -0.8 to +0.8 psi range. The static calibration curve is shown by Figure 3 and bears out the linear sensitivity variation as measured at the carrier amplifier output of 1.37 and 1.04 volts/psi for transducers 1 and 2, respectively, over a $\pm$0.8 psig pressure range.

4. Dynamic Calibration

For the dynamic calibration, a sinusoidal perturbation was introduced into the chamber by closing the static pressure port and

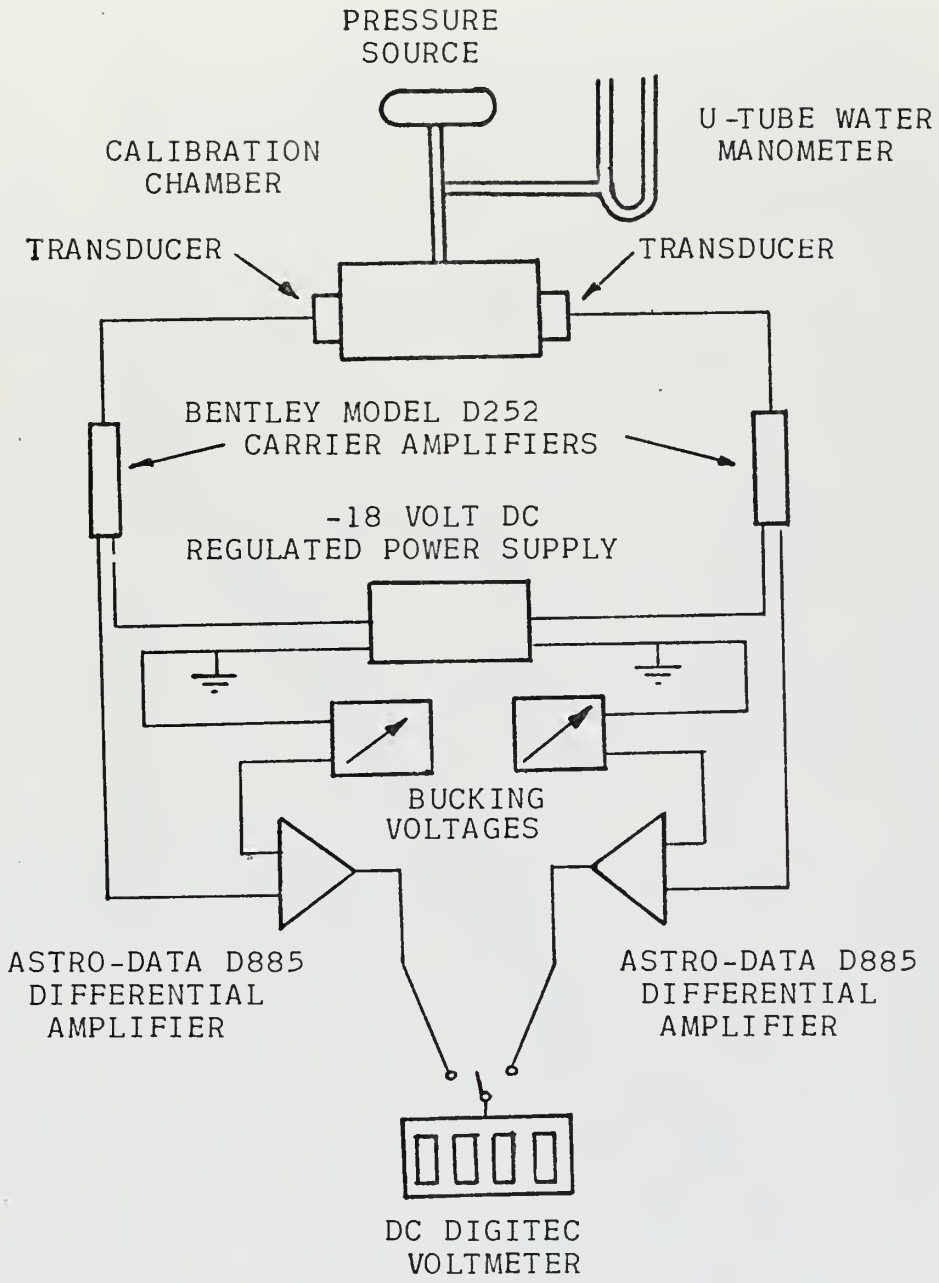


FIGURE 2

STATIC CALIBRATION INSTRUMENTATION

FIGURE 3

STATIC CALIBRATION CURVE

inserting an ID 75 University Sound acoustical driver unit driven by a Wavetek 114 signal generator which was amplified by a power amplifier. The acoustic driver unit was adjusted to operate at an input level of 13.5V RMS which corresponds to an oscillating pressure amplitude in the calibration chamber cavity of approximately 0.13 psi at 120 hertz. The carrier amplifier output was monitored with both a true RMS meter and a precision phasemeter, and visually monitored on a dual beam oscilloscope. The dynamic calibration instrumentation diagram is shown in Figure 4. The frequency was varied from 10 - 120 hertz in 5-hertz increments. Since the disturbance was introduced symmetrically into the chamber, there was no appreciable phase shift in oscillating measures at either end of the chamber; however, the sensitivity of transducer #2 was 0.787 of transducer #1 at every frequency increment.

F. EXPERIMENTATION

The data runs were made with the same system as was used for the dynamic calibration procedure with one exception; transducer #2 was remotely located from the calibration chamber through the use of nylon and stainless steel tubing. The brass diaphragm had a centered circular wrinkle which allowed brass shims to be inserted between the diaphragm and the plexiglass spacer in the transducer housing without hindering movement of the diaphragm. The wrinkle volume was estimated as 0.00211 $in.^3$ and the shims had an inside diameter of 0.523 in.: this allowed any desired transducer volume to be constructed. Frequencies of 10 - 120 hertz were investigated in 5-hertz increments for

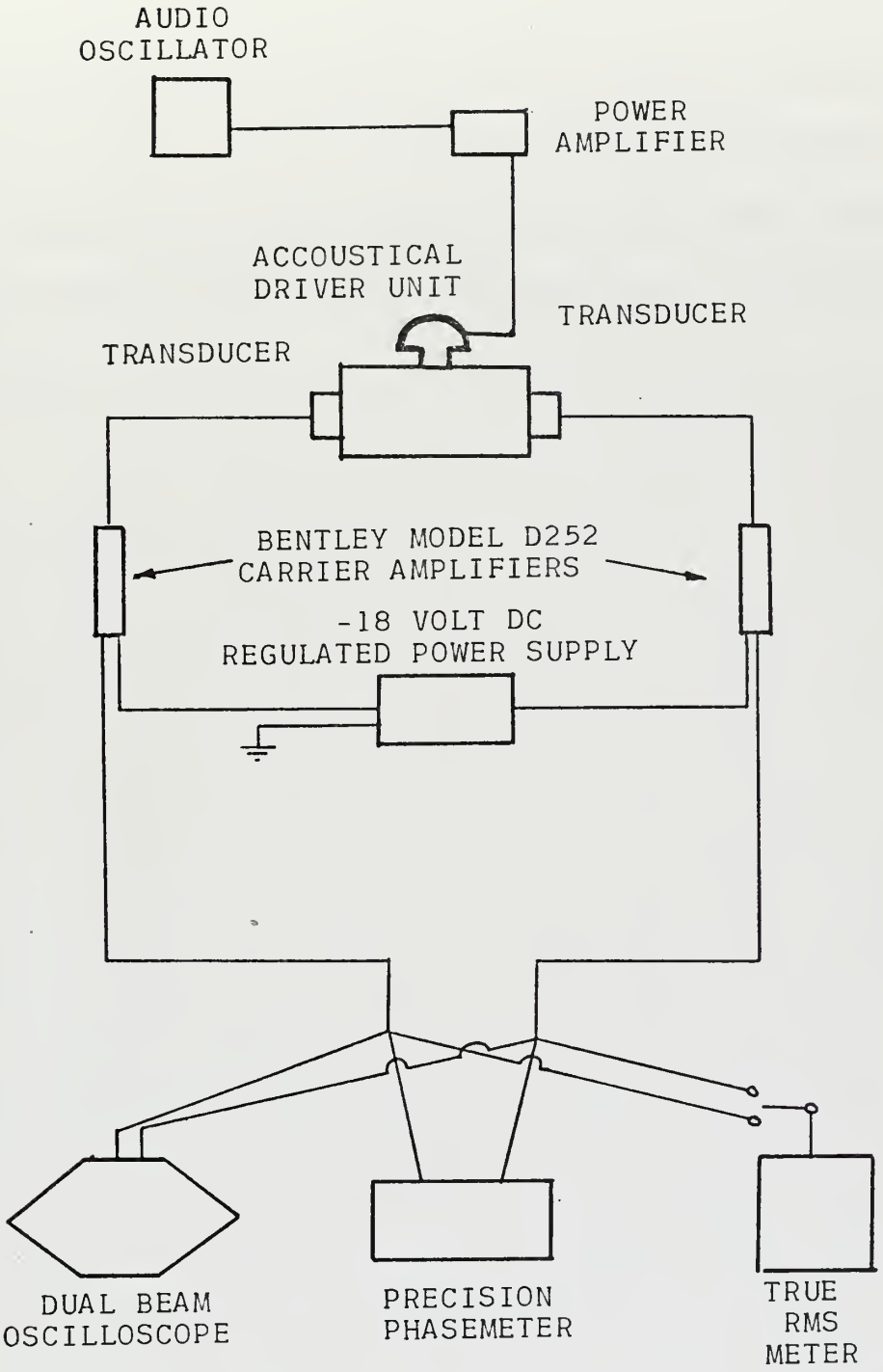


FIGURE 4

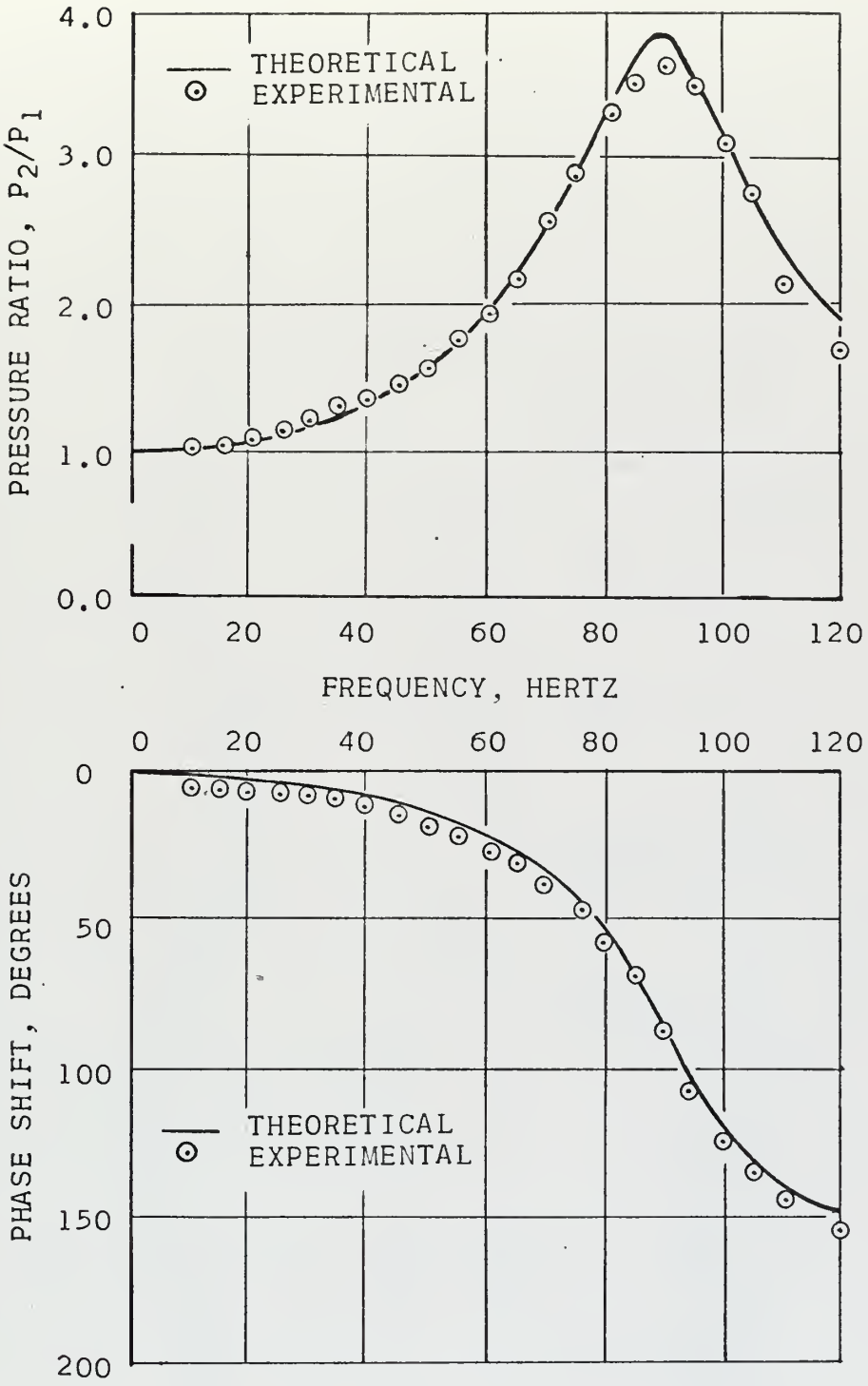
DYNAMIC CALIBRATION INSTRUMENTATION

different one-, two-, and three-tube configurations. The ratio of transducer output #2 divided by transducer output #1 was calculated and, because the sensitivity of transducer #2 was determined during dynamic calibration of transducer #1 as 0.787, the quotient was divided by 0.787 to normalize the output of transducer #2 with respect to transducer #1. This determined the frequency response (transfer function) of a given configuration.

III. DISCUSSION AND RESULTS

The computerized solution of Bergh's [1] prediction allowed quick and easy determination of the frequency response for a one-, two- or three-tube system, and could be easily modified for a greater number of tubes.

The one-tube solution generally followed the typical organ pipe solutions which produced sharp resonance peaks at many frequencies. When the resonance peaks did not occur, a heavily damped solution appeared. A solution was sought that would reduce the resonance peaks or raise the damped solution to the desired goal (1.00 ± 0.05); however, no such solution could be found for a 0 - 100 hertz range. The data runs did confirm Bergh's theoretical predictions for both pressure ratio and phase shift for a one-tube configuration, as can be seen by Figure 5. Therefore, a two-tube solution was examined in hopes that the pressure of an additional tube would counter the undesirable characteristics of the first tube. Such a configuration was found with the desired frequency response of 1.00 ± 0.05 from 10 to 100 hertz as shown by Figure 6. However, it was felt that the first tube in the system had a diameter that would result in the static orifice on the body being large enough to perturb the flow in the region of static pressure measurement. The two-tube configuration also verified Bergh's theoretical prediction of phase shift, but the pressure ratio was consistently lower (6%) than predicted for frequencies greater than 40 hertz (see Figure 7). A three-tube



TRANSDUCER VOLUME (CU. IN.)	0.0195
TUBE LENGTH (IN.)	28.0
TUBE DIAMETER (IN.)	0.078

FIGURE 5

SINGLE TUBE CONFIGURATION

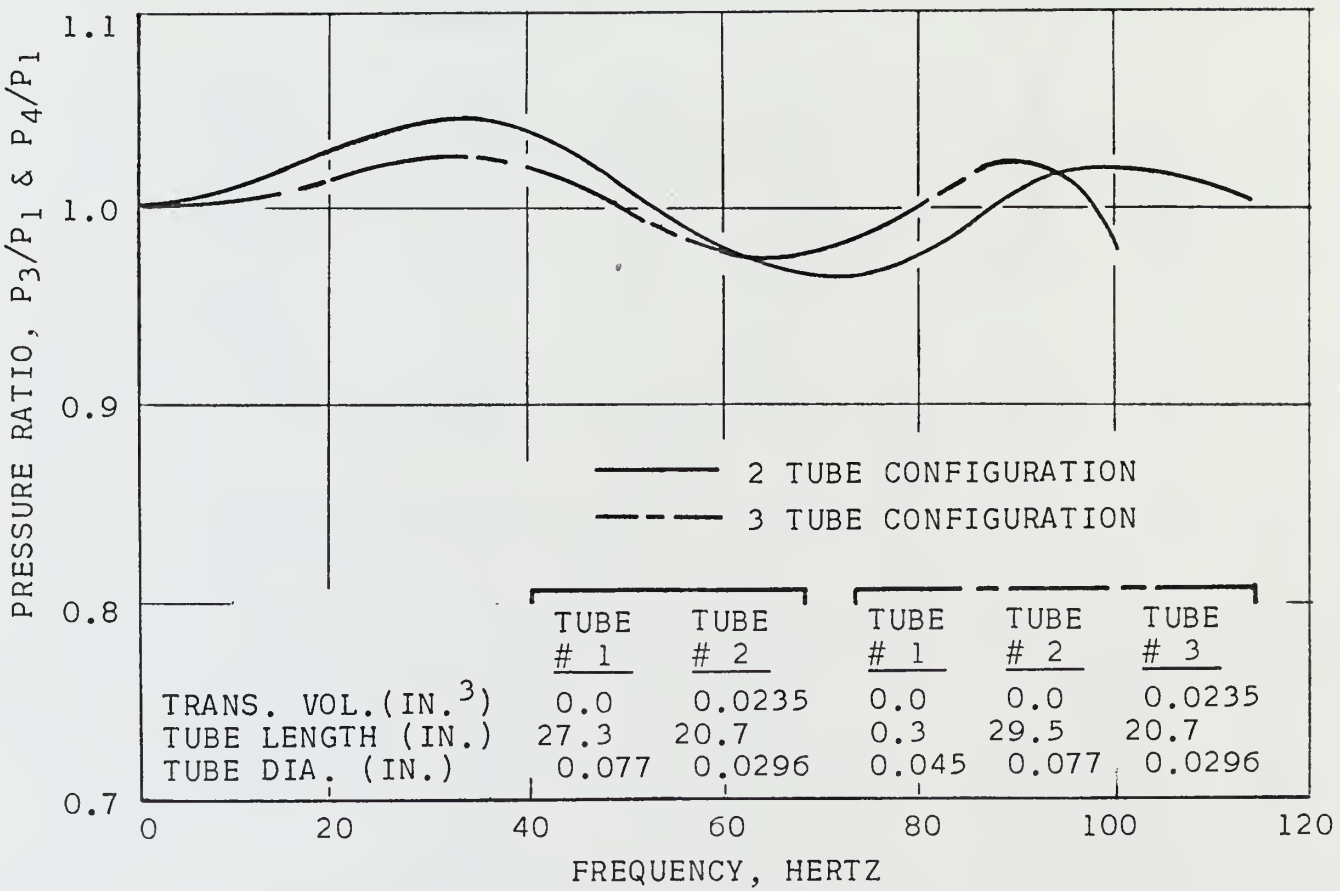
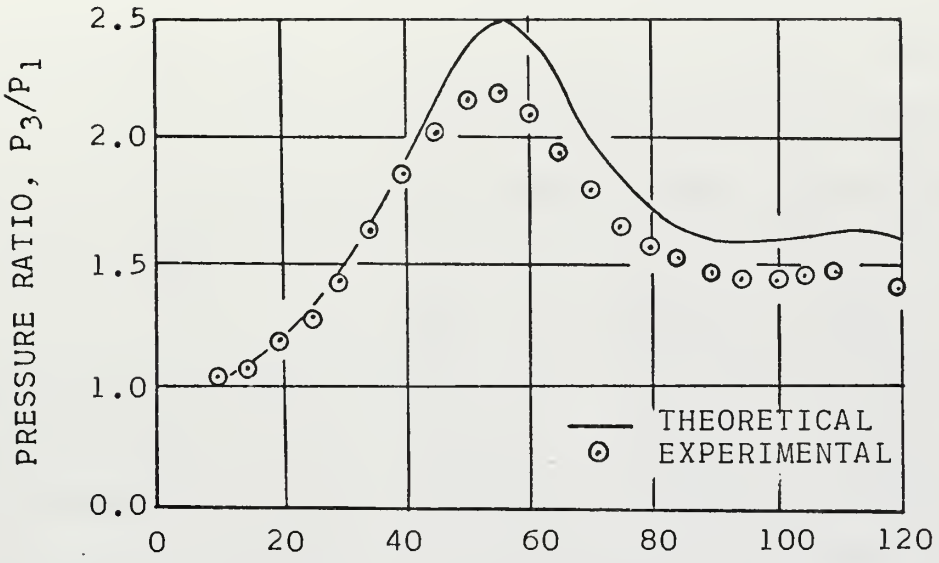
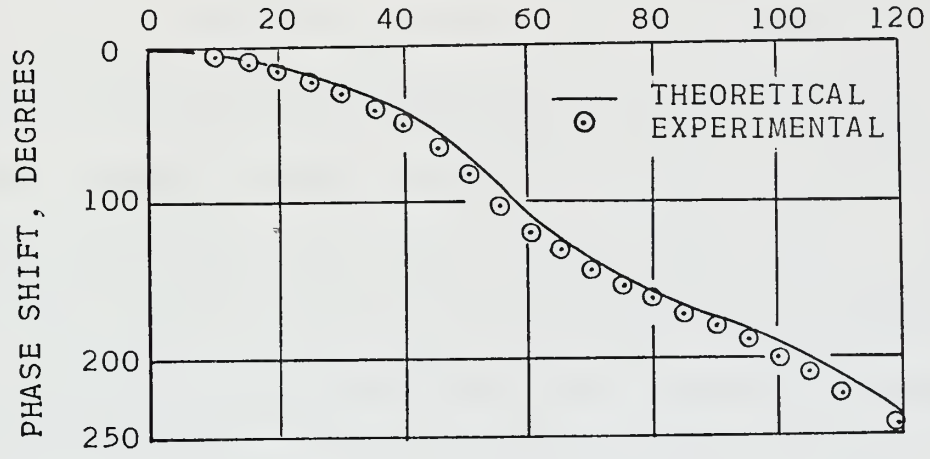


FIGURE 6

DESIRED THEORETICAL SOLUTIONS





	TUBE # 1	TUBE # 2
TRANS. VOL.(IN.^{3})	0.0	0.0238
TUBE LENGTH (IN.)	28.0	23.0
TUBE DIA. (IN.)	0.078	0.0465

FIGURE 7

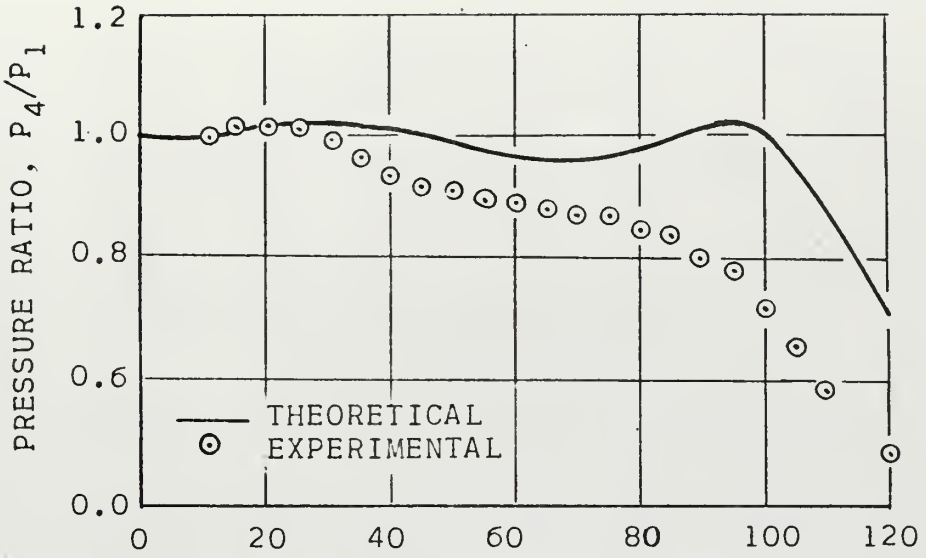
TWO TUBE CONFIGURATION

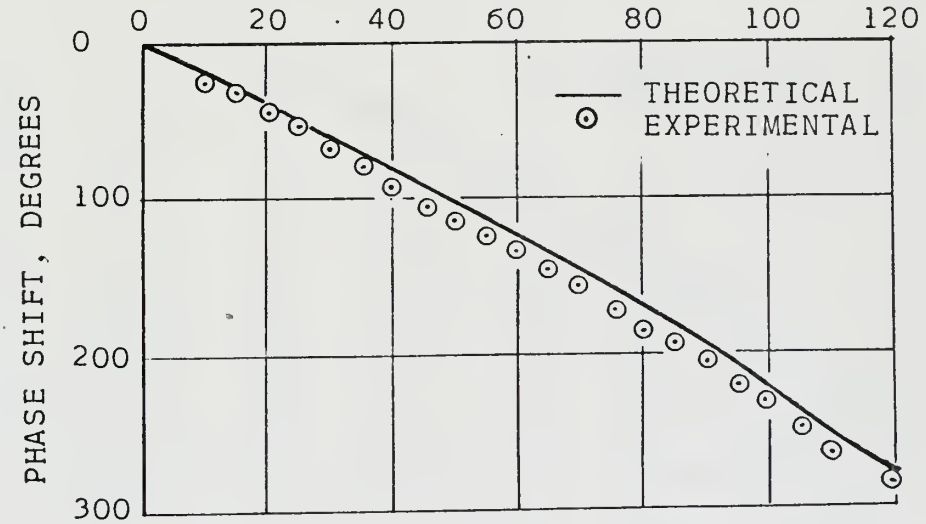
configuration was then sought in order to reduce the diameter of the first tube to an acceptable value (less than 0.05 inch). A solution which met all desired specifications (1.00 ± 0.03 over a 10 - 100 hertz range) was found (see Figure 6) and physically constructed in order to obtain experimental results to confirm the configuration selected. The configuration specifications were:

	Tube # 1	Tube # 2	Tube #3
Transducer volume ($in.^3$)	0.0	0.0	0.0238
Tube length (in.)	0.45	29.0	21.0
Tube diameter (in.)	0.0465	0.078	0.03

The three-tube solutions again confirmed the phase shift prediction; the experimental values were within 7% of their predicted values (see Figures 8a-d). However, as was the case with the two-tube solution, the three-tube experimental configuration produced pressure ratios less than those predicted by Bergh's solution for frequencies above 30 hertz with the values lower by as much as 30% (see Figures 8a-d). This characteristic made the theoretically acceptable solution (Figure 8a) of limited practical value since the experimental response was considerably below the prediction. Even though the actual solutions were not as predicted, Figure 10 shows trends comparable to those predicted by Bergh's solutions for identical configurations (Figure 9).

From Figures 8b-d, it was observed that changing the lengths of tubing raised or lowered the overall curve and a decrease in transducer volume (compare Figures 8a, b) tended to increase or raise the overall curve in the region of interest and decrease the slope above 80 hertz.

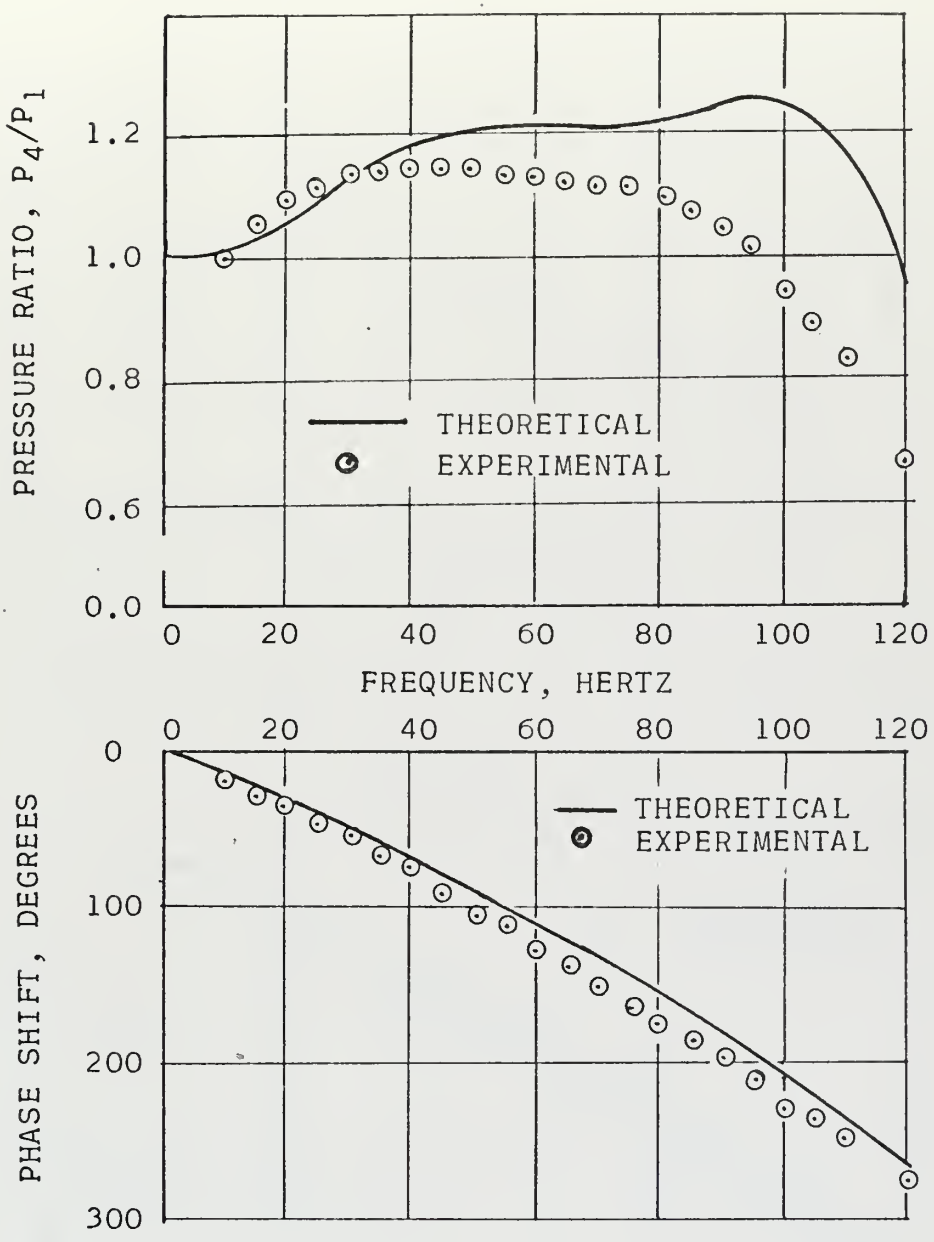




	TUBE # 1	TUBE # 2	TUBE # 3
TRANS. VOL.(IN.)	0.0	0.0	0.0238
TUBE LENGTH (IN.)	0.45	29.0	21.0
TUBE DIA.(IN.)	0.0465	0.078	0.03

FIGURE 8a

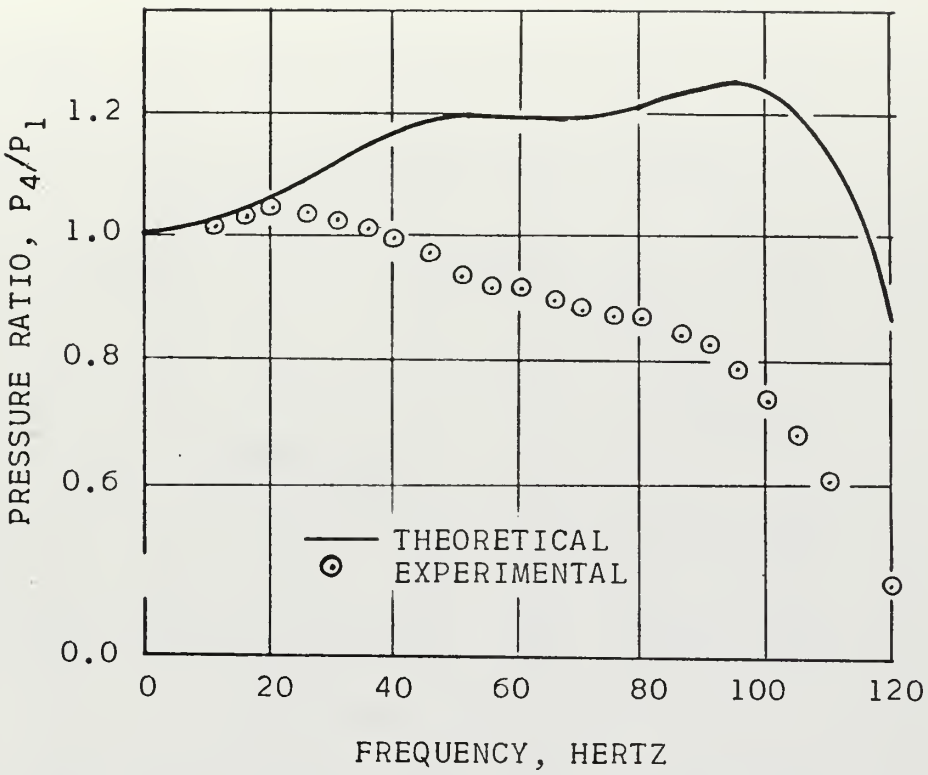
THREE TUBE CONFIGURATION

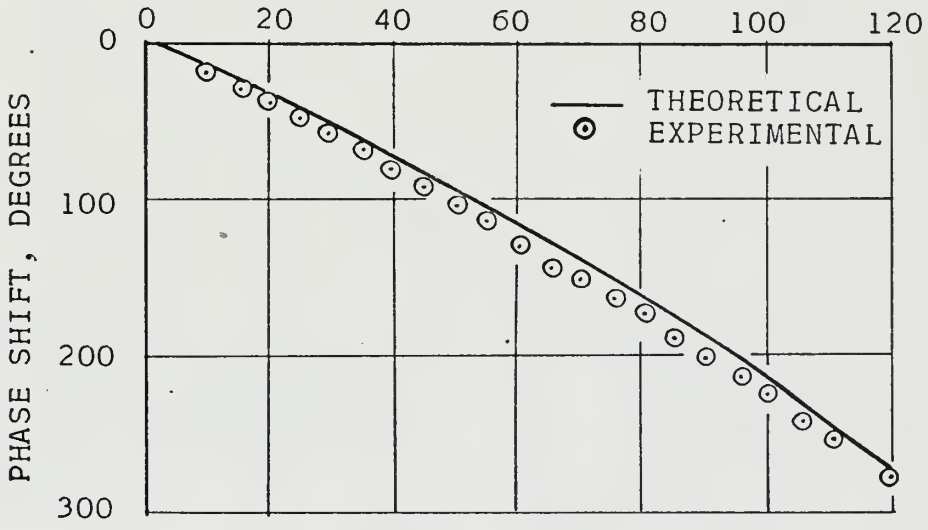


	TUBE # 1	TUBE # 2	TUBE # 3
TRANS. VOL.(IN.^{3})	0.0	0.0	0.0174
TUBE LENGTH (IN.)	0.45	28.5	20.5
TUBE DIA. (IN.)	0.0465	0.078	0.03

FIGURE 8b

THREE TUBE CONFIGURATION

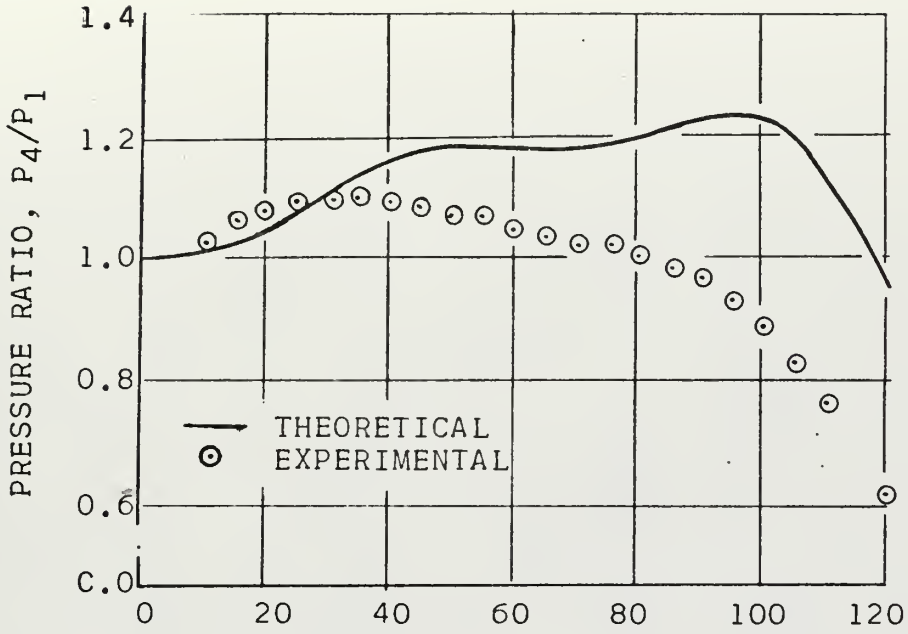


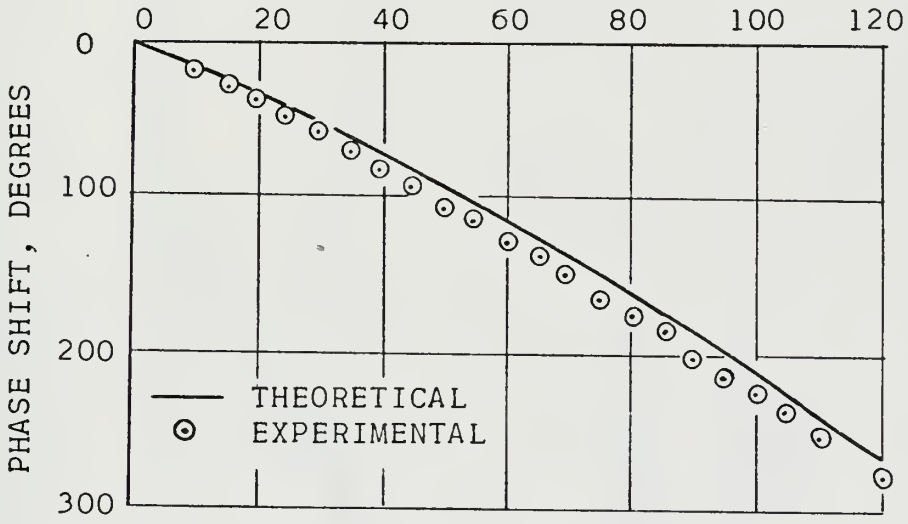


	TUBE # 1	TUBE # 2	TUBE # 3
TRANS. VOL.(IN.^{3})	0.0	0.0	0.0174
TUBE LENGTH (IN.)	0.45	29.0	21.0
TUBE DIA. (IN.)	0.0465	0.078	0.03

FIGURE 8c

THREE TUBE CONFIGURATION





	TUBE # 1	TUBE # 2	TUBE # 3
TRANS. VOL.(IN.^{3})	0.0	0.0	0.0174
TUBE LENGTH (IN.)	0.45	28.5	21.0
TUBE DIA. (IN.)	0.0465	0.078	0.03

FIGURE 8d

THREE TUBE CONFIGURATION

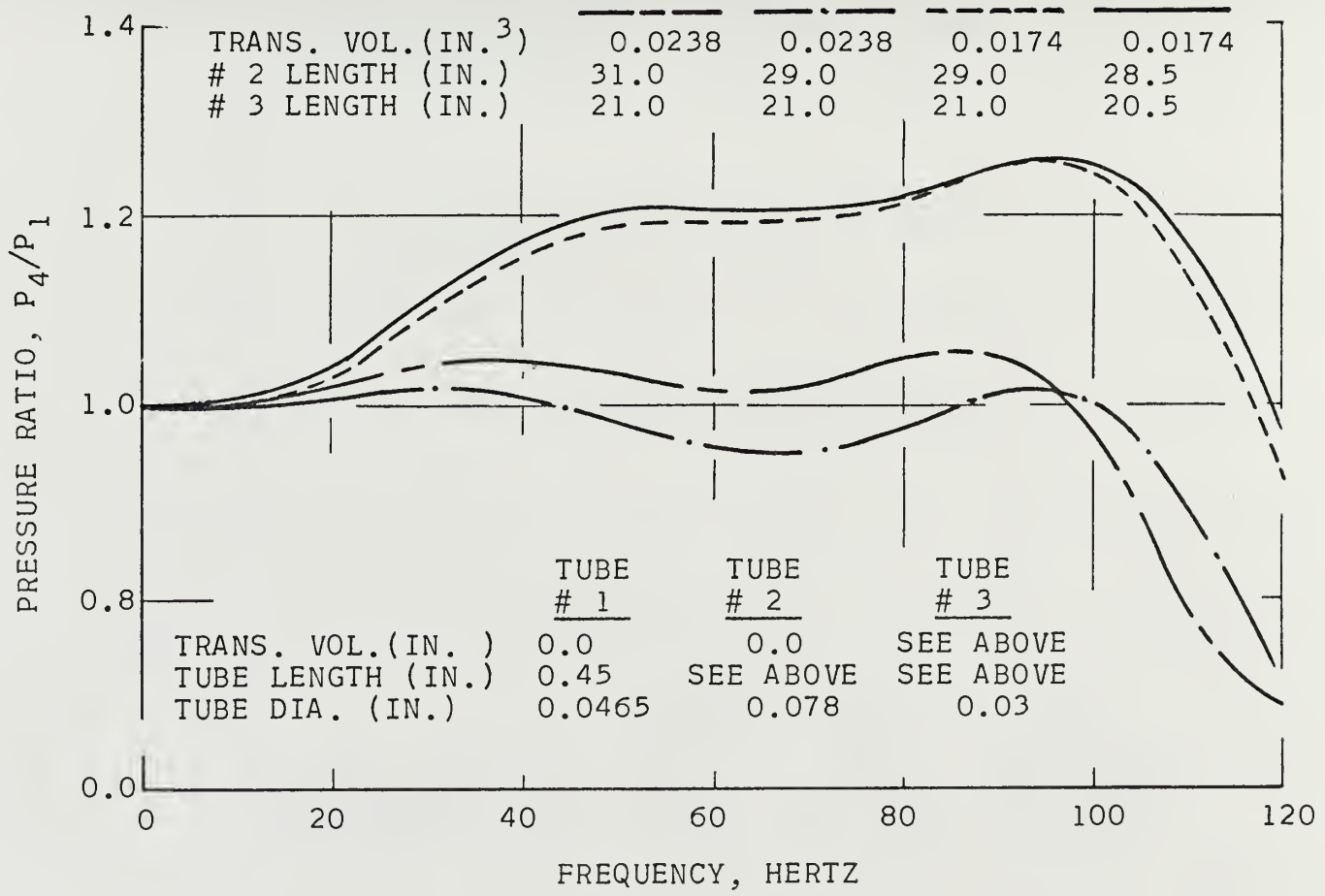


FIGURE 9

THEORETICAL TRENDS

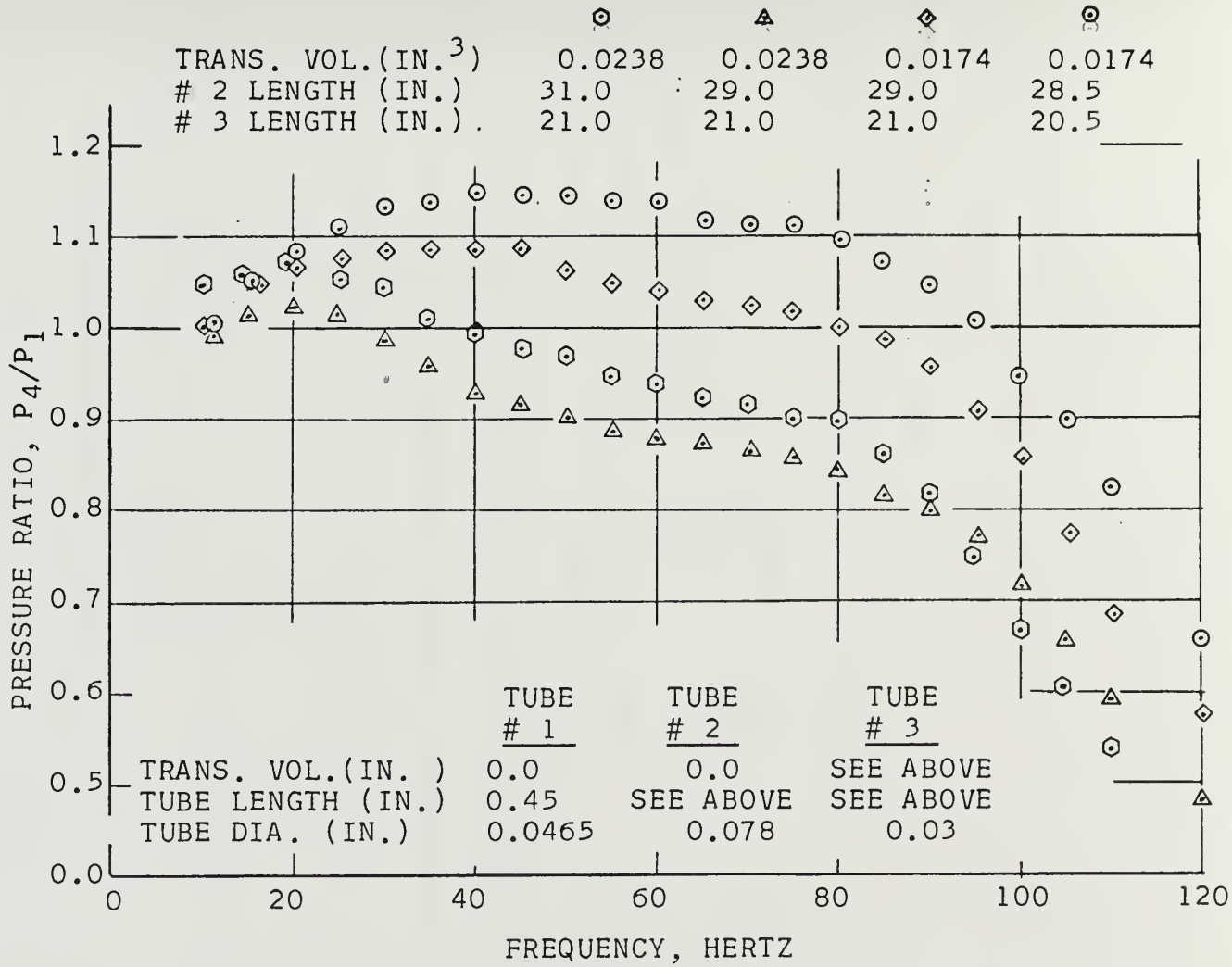


FIGURE 10

EXPERIMENTAL TRENDS

A small volume was tested and a possible solution of 1.00 ± 0.09 over a 10 - 95 hertz range was finally attained (see Figure 8d). This configuration appears acceptable for direct analog data processing in low-speed fields of interest. Much of the separated flow phenomenon is involved at non-dimensional frequencies or Strouhal numbers, S, less than 0.4 which would typically correspond to frequencies less than 100 hertz for a five-inch diameter circular cylinder at a tunnel speed of 100 feet per second. The solution configuration is specified below:

	Tube #1	Tube # 2	Tube # 3
Transducer volume ($in.^3$)	0.0	0.0	0.0174
Tube length (in.)	0.45	28.5	21.0
Tube diameter (in.)	0.0465	0.078	0.03

In addition to the tube lengths and transducer volumes, the three tube diameters were very important parameters when attaining the theoretical response desired. The diameter effects and trends were not examined, however, due to time and facility limitations and particularly due to the limited selection of commercial tube diameters available with acceptable inside diameter specifications.

The purpose for attaining a flat frequency response was to allow easy auto- and cross-correlation of a body in a low-speed unsteady flow employing a simple, low cost analog method shown by Figure 11. The cross-correlation coefficients, which relate the coherence of two physical measurements, say at stations (1) and (2), are in general defined for a specific value of time lag, τ, by:

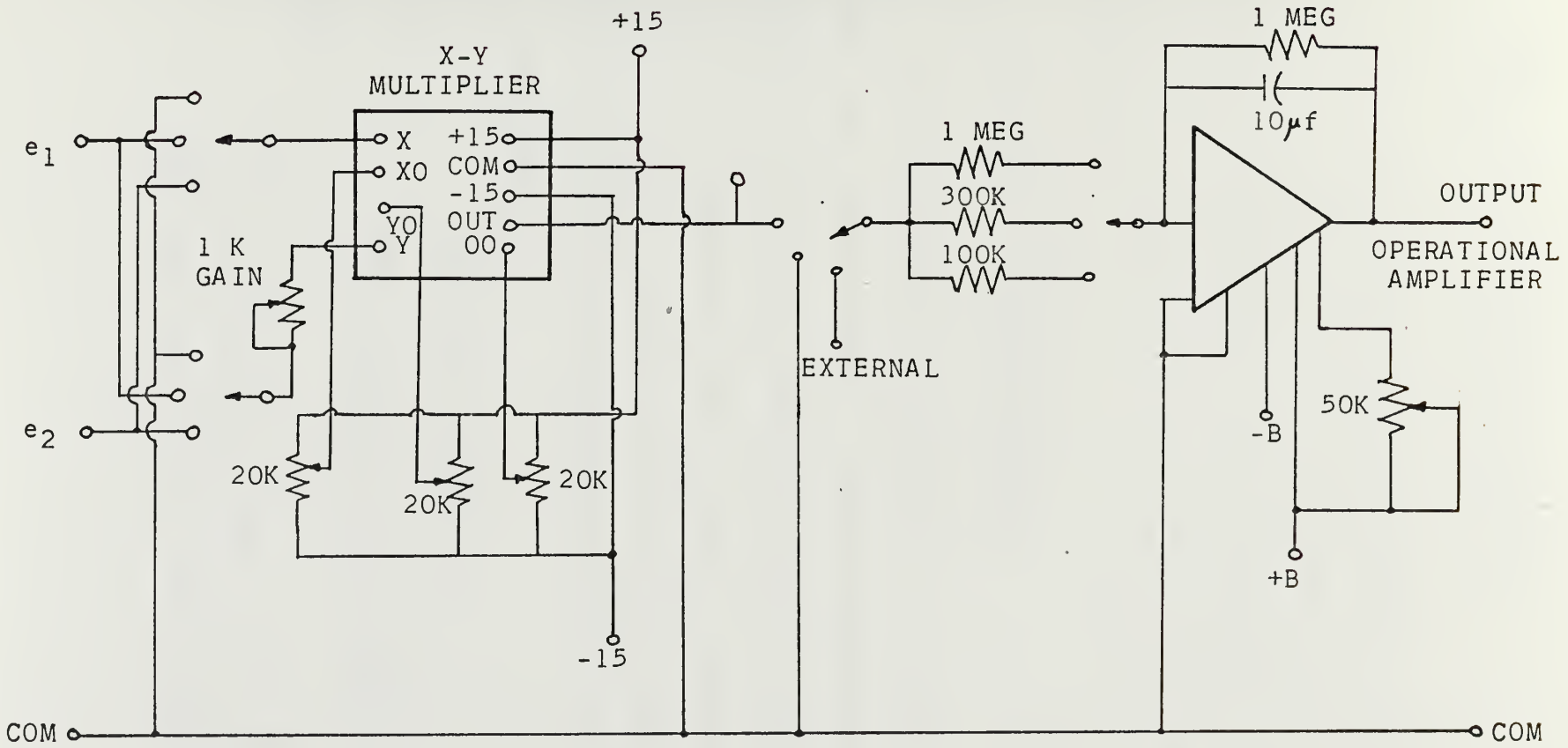


FIGURE 11

CROSS-CORRELATION CIRCUIT

$$R_{12}(\tau) = \frac{\langle e_1(t)\, e_2(t+\tau)\rangle}{\langle e_1^2\rangle^{1/2}\langle e_2^2\rangle^{1/2}}$$

However, the elementary analog correlation circuit shown in Figure 11 does not have a time lag capability and hence the benefit of simplicity is associated with a loss of information. Therefore, the information to be obtained must be at zero time lag as specified by equation (3):

$$R_{12}(0) = \frac{\langle e_1(0)\, e_2(0)\rangle}{\langle e_1^2\rangle^{1/2}\langle e_2^2\rangle^{1/2}}$$

Since the system in consideration, i.e., a remote pressure transducer system, can be likened to a typical transfer function system shown by Figure 1a, b, the cross-correlation inputs, e_1 and e_2, can be represented by the transducer outputs, p_1 and p_2. If the disturbance were of a sinusoidal nature as it was for the laboratory experiment, then the two measuring stations become strictly functions of the frequency, .

Suppose:

$$p_1 = p_{o1} \sin \omega t$$

$$p_2 = p_{o2} \sin (\omega t - \Theta)$$

then:

$$\hat{p}_1(t) = p_{o1} G_1(\omega) \sin (\omega t - \phi_1)$$

$$\hat{p}_2(t) = p_{o2} G_2(\omega) \sin (\omega t - \Theta - \phi_2)$$

Substitution into equation (3) will yield a cross-correlation coefficient as follows:

$$R_{12}(0) = \frac{G_1(\omega)\, G_2(\omega)\, \cos(\Theta + \phi_2 - \phi_1)}{G_1(\omega)\, G_2(\omega)}$$

From equation (4) it can be seen that for the case of a pair of information signals at a unique circular frequency, ω, with the respective transfer functions $G_1(\omega)$ and $G_2(\omega)$ equivalent, then:

$$R_{12}(0) = \cos \Theta$$

and a flat frequency response is not necessary. It is only necessary to have identical transfer functions used with both signals.

However, this analysis eliminates one of the most important types of flow fields, the unsteady random signal such as that produced by flow separation from a bluff body. In such cases the cross-correlation coefficient can no longer be simplified to equation (5). Instead, because of its reliance on G as a function of ω, the output of the cross-correlation system becomes:

$$\hat{R}_{12}(0) = \frac{\int_0^\infty G_1(\omega)\, G_2(\omega)\, \Phi_{12}(\omega)\, d\omega}{\left\{\left[\int_0^\infty G_1^2(\omega)\, \Phi_{11}(\omega) d\omega\right]\left[\int_0^\infty G_2^2(\omega)\, \Phi_{22}(\omega) d\omega\right]\right\}^{1/2}} \quad (6)$$

where

Φ_{11} = power spectral density of signal 1

Φ_{22} = power spectral density of signal 2

Φ_{12} = co-spectral density of signals 1 and 2

At the input of the transducer system, the cross-correlation coefficient is not a function of G and thus reduces to the form:

$$R_{12}(0) = \frac{\int_0^\infty \Phi_{12}(\omega)\, d\omega}{\left\{\left[\int_0^\infty \Phi_{11}(\omega)\, d\omega\right]\left[\int_0^\infty \Phi_{22}(\omega)\, d\omega\right]\right\}^{1/2}} \tag{7}$$

In order for (6) to equal (7) for any random signal, the following relationship is obviously necessary.

$$G_1(\omega) = G_2(\omega) = 1.0 \tag{8}$$

Should (8) be the case, then,

$$R_{12}(0)_{\text{input}} = R_{12}(0)_{\text{output}}$$

and the system no longer relies on the gain of the transducer system. A complete derivation of the cross-correlation equations may be found in Appendix C.

Because of the flat frequency response, the collected data may be inputted directly to the cross-correlation circuit shown in Figure 11 and the output monitored by either a D.C. voltmeter or an x-y plotter to obtain quantities $\langle e_1 e_2 \rangle$, $\langle e_1^2 \rangle^{\frac{1}{2}}$, and $\langle e_2^2 \rangle^{\frac{1}{2}}$, which allows a simple calculation of the cross-correlation coefficient at zero time lag.

IV. CONCLUSION AND RECOMMENDATIONS

Although the breakdown of Bergh's theory seems to be directly proportional to the number of tubes in the configuration, it does predict fairly accurately the trends that each parameter impresses on a system. There is, therefore, a good possibility of obtaining a flatter frequency response than the one obtained in Figure 8d. Time limitations required the termination of the experiment and the three-tube configuration was in no way completely examined.

It should be noted that the flat frequency response traits considered herein applied to a fairly restrictive range of frequencies, namely less than 100 hertz. The processing of a broader class of signals, i.e., a higher range of frequencies, will probably require the utilization of several steps or procedures, including:

a. Recording of the analog form of the data signals on a magnetic tape recorder.

b. Digitizing the analog signals using a common time base or clock, and

c. Processing the digitized data by means of a digital computer.

Portions of this procedure have been within the scope of the school's experimental facilities within recent times, cf., Jesberg [7] ; however, new equipment additions or replacements make this former technique no longer practical until a repeat is done of the work by Jesberg [7] .

It is observed from Figures 7 and 8a-d that the theory under-predicts the pressure ratio for both two- and three-tube configurations, yet the phase prediction is very close to the correct value.

The following recommendations are therefore made:

1.) Further experimentation of parameter effects in order to obtain a flatter frequency response.

2.) Possible modification of the computer program to allow compensation for the difference between the actual and theoretical response.

APPENDIX A

THEORETICAL RESPONSE OF A REMOTELY LOCATED PRESSURE TRANSDUCER SYSTEM

Bergh's theoretical model applies to any number of transmitting tubes in a cascaded tube system as shown by Figure 1b; however, many assumptions are made in order to reduce the governing equations to a workable form. These assumptions are as follows:

a) the sinusoidal disturbances are very small:

b) the inner diameter of the tubing is small with respect to its length:

c) laminar flow exists throughout the system:

d) the unsteady disturbances are perturbations imposed on the average values on the parameters indicated below:

$$
\begin{aligned}
&1)\quad \bar{p} = p_o + pe^{iwt} && \text{Pressure}\\
&2)\quad \bar{\rho} = \rho_o + \rho e^{iwt} && \text{Density}\\
&3)\quad \bar{T} = T_o + Te^{iwt} && \text{Temperature}\\
&4)\quad \bar{u} = u_o + ue^{iwt} && \text{Axial Velocity}\\
&5)\quad \bar{v} = v_o + ve^{iwt} && \text{Radial Velocity}
\end{aligned}
\qquad (A1)
$$

These assumptions allow the governing equations to be reduced to the following forms:

Navier-Stokes Equations

$$-\frac{1}{\rho_0}\frac{\partial p}{\partial x}+\mu\rho_0\left[\frac{\partial^2 u}{\partial r^2}+\frac{1}{r}\frac{\partial u}{\partial r}\right]=i\omega u \tag{A2}$$

$$-\frac{\partial p}{\partial r}=0 \tag{A2a}$$

Continuity Equation

$$-\rho_0\left[\frac{\partial u}{\partial x}+\frac{\partial v}{\partial r}+\frac{v}{r}\right]=i\omega\rho \tag{A3}$$

Perfect Gas Law

$$\frac{\gamma}{a_0^2}\left[1+\frac{\rho_0 T}{T_0\rho}\right]=\rho \tag{A4}$$

Energy Equation

$$\lambda\left[\frac{\partial^2 T}{\partial r^2}+\frac{1}{r}\frac{\partial T}{\partial r}\right]=i\omega\rho+i\omega\rho_0 g C_p T \tag{A5}$$

Since the equations are now partial differential equations, boundary conditions can now be specified:

a) At r = R, the tube's inside wall,

1) u(X,R) = 0

2) v(X,R) = 0

3) T(X,R) = 0

b) At r = 0, the tube center,

1) $v(X,0) = 0$

2) $u(X,0) =$ finite

3) $T(X,0) =$ finite

4) $p(X,0) =$ finite

5) $p(X,0) =$ finite

From equation (A2a) it is evident that $p = p(x)$, which allows a separation of variables technique.

assume:

$$T = f(x)\, h(z) \tag{A6}$$

where:

$$\alpha = i^{3/2} R \left(\frac{\rho_0 \omega}{\mu}\right)^{1/2}$$

$$P_r = \frac{\mu g c_p}{\lambda} = \text{PRANDTL NUMBER}$$

$$z = \frac{\alpha r}{R} P_r^{1/2}$$

Equation (A5) takes on a Bessel equation form of the following type in this type of solution:

$$h(z) = C_1 J_0(z) + C_2 Y_0(z) + \frac{p}{\rho g c_p} \frac{1}{f(x)} \tag{A7}$$

Apply boundary conditions a3 and b3

$$f(x) = -\frac{1}{C_1 J_0(\alpha P_r^{1/2})} \frac{p(x)}{\rho_0 g c_p} \tag{A8}$$

Using (A7) and (A8) in (A6) yields:

$$\rho = \frac{\gamma}{a_0^2} p \left\{ 1 - \frac{\gamma - 1}{\gamma} \left[1 - \frac{J_0\left(\frac{r}{R}\alpha P_r^{1/2}\right)}{J_0\left(\alpha P_r^{1/2}\right)} \right] \right\} \tag{A9}$$

Similar methods using boundary conditions a1 and b2 can be applied to solve equation (1) as given below:

$$u = \left[\frac{J_0\left(\frac{r}{R}\alpha\right)}{J_0(\alpha)} - 1 \right] \frac{1}{i\omega\rho_0} \frac{dp}{dx} \tag{A10}$$

Substituting equations (A9) and (A10), integrating with respect to r, and applying boundary condition a2 will put equation (A7) in the form:

$$-F(x) = \frac{\omega^2}{a_0^2} \gamma \frac{R^2}{2} p \left\{ 1 + \frac{\gamma - 1}{\gamma} \frac{J_2\left(\alpha P_r^{1/2}\right)}{J_0\left(\alpha P_r^{1/2}\right)} \right\} - \frac{R^2}{2} \frac{d^2 p}{dx^2} \frac{J_2(\alpha)}{J_0(\alpha)}$$

Since $v(X,0) = 0$ implies $F(X) = 0$,

$$\frac{\omega^2}{a_0^2} \gamma p \left[1 + \frac{\gamma - 1}{\gamma} \frac{J_2\left(\alpha P_r^{1/2}\right)}{J_0\left(\alpha P_r^{1/2}\right)} \right] - \frac{J_2(\alpha)}{J_0(\alpha)} \frac{d^2 p}{dx^2} = 0$$

The above equation can be solved for the homogeneous solution:

$$p = A e^{\phi x} + B e^{-\phi x}$$

where

$$\phi = \frac{\omega^2}{a_0^2} \frac{J_0^{1/2}(\alpha)}{J_2^{1/2}(\alpha)} \gamma^{1/2} \left[1 + \frac{\gamma - 1}{\gamma} \frac{J_2\left(\alpha P_r^{1/2}\right)}{J_0\left(\alpha P_r^{1/2}\right)} \right]^{1/2}$$

The coefficients A and B can be determined only after the boundary conditions for both ends of the tube have been specified. It should also be noted here that the Bessel functions in the equations are complex numbers since $\alpha = \alpha(i^{3/2} y)$. This is discussed further in Appendix B.

Two additional assumptions must now be made if the solution is to cover an N-tube, N volume configuration:

c) the pressure and density in the instrument volumes are time dependent only

d) the pressure expansion in the instrument volume is a polytropic process described by

$$\frac{\bar{p}_v}{\bar{\rho}_v^{\,k}} = \text{constant}$$

The constants A and B are now determined in the following procedure.

For any tube j,

at $x_j = 0$

$$p_{j-1} = A_j + B_j \tag{A11}$$

at $x_j = l_j$

$$p_j = A_j e^{\phi_j l_j} + B_j e^{-\phi_j l_j}$$

$$u_j = \frac{i\phi_j}{\omega \rho_{s_j}} \left\{ \frac{J_0\left(\frac{\alpha_j R_j}{r}\right)}{J_0(\alpha_j)} - 1 \right\} \left[A_j e^{\phi_j l_j} - B_j e^{-\phi_j l_j} \right] \tag{A12}$$

Equations (A11 and (A12) allow solution for A_j and B_j.

$$A_j = \frac{p_j - p_{j-1} e^{-\phi_j L_j}}{e^{\phi_j L_j} - e^{-\phi_j L_j}}$$

$$B_j = \frac{p_{j-1} e^{\phi_j L_j} - p_j}{e^{\phi_j L_j} - e^{-\phi_j L_j}}$$

The mass leaving the tube can now be calculated:

$$m_{j1} = \int_0^{R_j} \rho_{s_j} u_j \, 2\pi r \, dr =$$

$$\frac{\pi R_j^2 \phi_j J_2(\alpha_j)}{i \omega J_0(\alpha_j)} \left[A_j e^{\phi_j L_j} - B_j e^{-\phi_j L_j} \right]$$

For any tube j + 1,

$$\text{at } x_{j+1} = 0 \qquad \text{(A13)}$$

$$p_j = A_{j+1} + B_{j+1}$$

$$\text{at } X_{j+1} = L_{j+1}$$

$$p_{j+1} = A_{j+1} e^{\phi_{j+1} L_{j+1}} + B_{j+1} e^{-\phi_{j+1} L_{j+1}} \qquad \text{(A14)}$$

$$u_{j0} = \frac{i \phi_{j+1}}{\omega \rho_{s_{j+1}}} \left\{ \frac{J_0\left(\frac{\alpha_{j+1} R_{j+1}}{r}\right)}{J_0(\alpha_{j+1})} - 1 \right\} + \left[A_{j+1} - B_{j+1} \right]$$

The mass leaving tube j+1 is now calculated:

$$m_{j0} = \int_0^{R_{j+1}} \rho_{s_{j+1}} u_{j0} \, 2\pi r \, dr =$$

$$\frac{\pi R_{j+1}^2 \phi_{j+1}}{i \omega} \frac{J_2(\alpha_{j+1})}{J_0(\alpha_{j+1})} \left(A_{j+1} - B_{j+1} \right)$$

Equations (A13) and (A14) allow solution for A_{j+1} and B_{j+1}

$$A_{j+1} = \frac{p_{j+1} - p_j e^{-\phi_{j+1} L_{j+1}}}{e^{\phi_{j+1} L_{j+1}} - e^{-\phi_{j+1} L_{j+1}}}$$

$$B_{j+1} = \frac{p_j e^{\phi_{j+1} L_{j+1}} - p_{j+1}}{e^{\phi_{j+1} L_{j+1}} - e^{-\phi_{j+1} L_{j+1}}}$$

The mass variation within the instrument volume must equal the difference in the mass leaving tube j and entering j+1, namely:

$$\frac{dm_v}{dt} = e^{i\omega t} p_j \frac{i\omega\gamma}{a_o^2} V_{v_j} \left(\sigma_j + \frac{1}{K_j}\right) = (m_{j_1} - m_{j_0}) e^{i\omega t} \qquad \text{(A15)}$$

Substitution of the pressure coefficients into (A15) and recalling the definitions

$$\cosh \omega t = \frac{e^{\omega t} - e^{-\omega t}}{2} \quad \text{and} \quad \sinh \omega t = \frac{e^{\omega t} + e^{-\omega t}}{2}$$

the final pressure ratio prediction is obtained.

$$\frac{p_j}{p_{j-1}} = \left[\cosh(\phi_j L_j) + \frac{\omega^2 \gamma}{a_o^2} \frac{V_{v_j}\left(\sigma_j + \frac{1}{K_j}\right)}{\pi R_j^2 \phi_j} \frac{J_0(\alpha_j)}{J_2(\alpha_j)} \sinh(\phi_j L_j) \right.$$
$$+ \frac{\pi R_{j+1}^2}{\pi R_j^2} \frac{\phi_{j+1}}{\phi_j} \frac{J_2(\alpha_{j+1})}{J_0(\alpha_{j+1})} \frac{J_0(\alpha_j)}{J_2(\alpha_j)} \frac{\sinh(\phi_j L_j)}{\sinh(\phi_{j+1} L_{j+1})} \times$$
$$\left. \left\{ \cosh(\phi_{j+1} L_{j+1}) - \frac{p_{j+1}}{p_j} \right\} \right]^{-1}$$

APPENDIX B

COMPUTERIZATION OF THE THEORETICAL RESPONSE OF A REMOTE PRESSURE TRANSDUCER SYSTEM

A. Computer Program Development

In Bergh's theoretical development (Appendix A), the Bessel function parameter, α, contains the imaginary term, $i^{3/2}$, which can easily be represented by the Kelvin functions Ber, Bei, Ber_1, and Bei_1. These functions were used in the program in the form of an infinite power series and terminated when the terms become smaller than 10^{-10}. The series expansions were taken from McLachlan [4] and altered into the form below:

$$J_o(\alpha) = \text{ber } y + i \text{ bei } y \tag{B1}$$

$$\alpha = i^{3/2} R \left(\frac{\rho_o \omega}{\mu}\right)^{1/2} = i^{3/2} y$$

$$\text{ber } y = 1 - \frac{y^4}{(2\cdot4)^2} + \frac{y^8}{(2\cdot4\cdot6\cdot8)^2} - \frac{y^{12}}{(2\cdot4\cdot6\cdot8\cdot10\cdot12)^2} + \cdots$$

$$\text{bei } y = \frac{y^2}{2} - \frac{y^6}{(2\cdot4\cdot6)^2} + \frac{y^{10}}{(2\cdot4\cdot6\cdot8\cdot10)^2} - \cdots$$

$$J_1(\alpha) = \text{ber}_1 Y + i\ \text{bei}_1 Y$$

$$\text{ber}_1 Y = -\frac{Y}{2\sqrt{2}}\left[1 + \frac{Y^2}{2\cdot 2^2} - \frac{Y^4}{2^4\cdot 2^2\cdot 3} - \frac{Y^6}{2^6\cdot(2\cdot 3)^2\cdot 4} + \cdots\right] \tag{B2}$$

$$\text{bei}_1 Y = -\frac{Y}{2\sqrt{2}}\left[1 - \frac{Y^2}{2\cdot 2^2} - \frac{Y^4}{2^4\cdot 2^2\cdot 3} + \frac{Y^6}{2^6\cdot(2\cdot 3)^2\cdot 4} + \cdots\right]$$

$$J_2(\alpha) = \frac{2\,J_1(\alpha)}{Y} - J_0(\alpha) \tag{B3}$$

B. Computer Program Operation

The computer program was designed primarily for use on a time-sharing system remote terminal where quick output could be obtained for a given input. However, it may also be modified for batch processing as explained below. The computer program allows selection of either a 1, 2 or 3 tube configuration by the operator and prints out the pressure ratio and phase shift for multiples of 5 hertz from 10 to 120 hertz. The flowchart is given in Figure (B1).

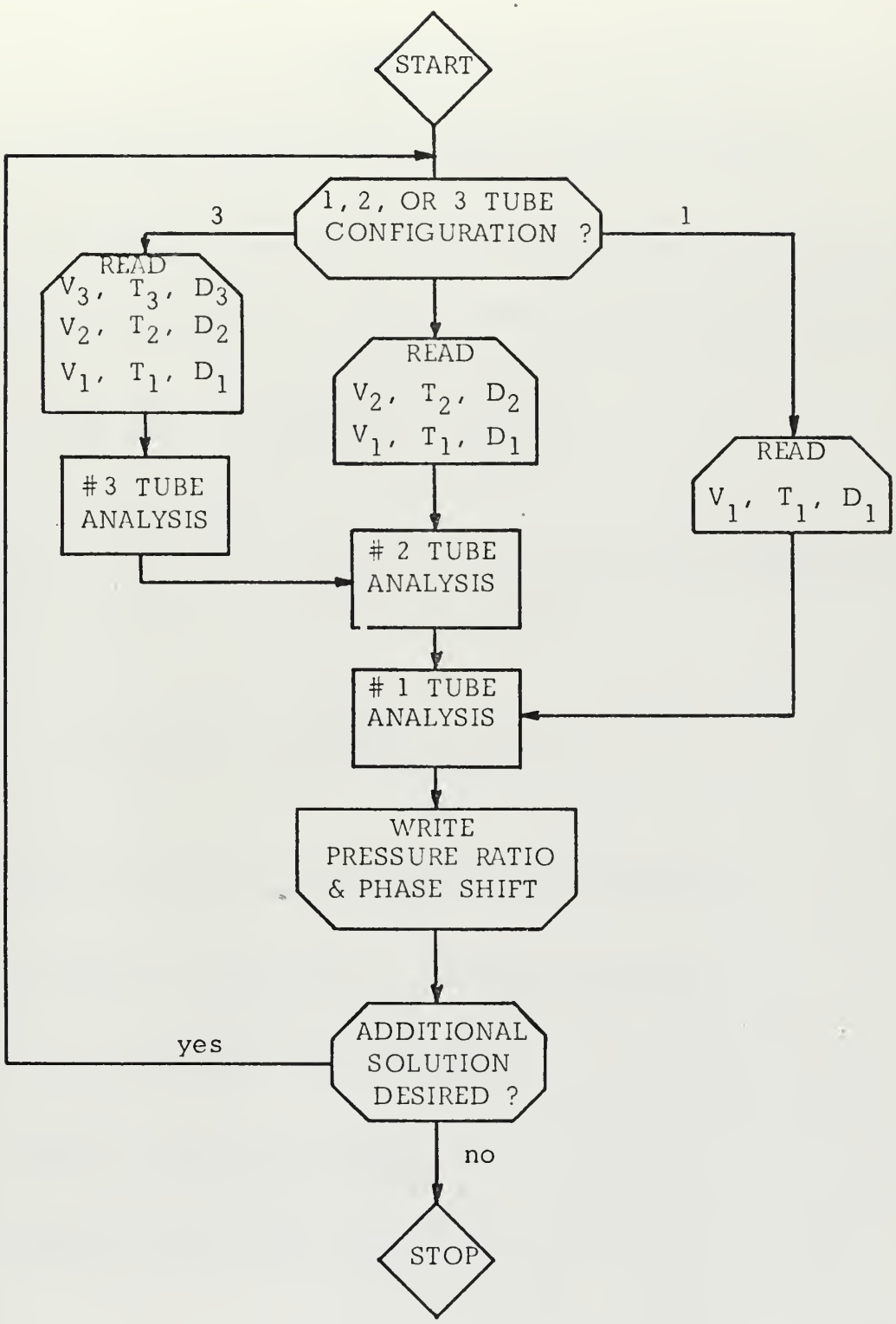


FIGURE B1

COMPUTER PROGRAM FLOWCHART

APPENDIX C

CROSS-CORRELATION OF A RANDOM UNSTEADY SIGNAL

The cross-correlation coefficient may be defined in its most general form similar to methods described in Bendat and Piersol [8].

$$R_{12}(t) = \frac{\langle e_1(t)\, e_2(t+\tau)\rangle}{\langle e_1^2\rangle^{1/2}\, \langle e_2^2\rangle^{1/2}} \tag{C1}$$

However, because of the zero time lag limitation of the analog circuit shown in Figure 11, this reduces to the form:

$$R_{12}(0) = \frac{\langle e_1 e_2\rangle}{\langle e_1^2\rangle^{1/2}\, \langle e_2^2\rangle^{1/2}} \tag{C2}$$

For the system input, the following terms are defined as:

$$\begin{aligned} \langle e_1 e_2\rangle &= \lim_{T\to\infty} \frac{1}{2T}\int_{-T}^{T} e_1(t)\, e_2(t)\, dt \\ &= \int_0^\infty \Phi_{12}(\omega)\, d\omega \end{aligned} \tag{C3}$$

$$\langle e_1^2\rangle = \int_0^\infty \Phi_{11}(\omega)\, d\omega$$

$$\langle e_2^2\rangle = \int_0^\infty \Phi_{22}(\omega)\, d\omega$$

Φ_{11} = power spectral density of signal 1

Φ_{22} = power spectral density of signal 2

Φ_{12} = co spectral density of signals 1 and 2

After passing through the system, the quantities have a transfer function imposed on their true output, and the following terms are defined:

$$\hat{e}_1(\omega) = G_1(\omega)\, e^{-i\phi}\, e_1(\omega)$$

$$e_1(\omega) = A_1 e^{-i\omega t} \tag{C4}$$

thus:

$$\begin{aligned} \langle \hat{e}_1 \hat{e}_2 \rangle &= \int_0^\infty G_1(\omega)\, G_2(\omega)\, \Phi_{12}(\omega)\, d\omega \\ \langle \hat{e}_1^2 \rangle &= \int_0^\infty G_1^2(\omega)\, \Phi_{11}(\omega)\, d\omega \\ \langle \hat{e}_2 \rangle &= \int_0^\infty G_2^2(\omega)\, \Phi_{22}(\omega)\, d\omega \end{aligned} \tag{C5}$$

A relationship between the output and input cross-correlations may be obtained by direct substitution of (C3) and (C5) into (C2), yielding:

$$\frac{\int_0^\infty \hat{\Phi}_{12}(\omega)\, d\omega}{\left[\int_0^\infty \hat{\Phi}_{11}(\omega)\, d\omega\right]\left[\int_0^\infty \hat{\Phi}_{22}(\omega)\, d\omega\right]} = \tag{C6}$$

$$\frac{\int_0^\infty G_1(\omega)\, G_2(\omega)\, \Phi_{12}(\omega)\, d\omega}{\left\{\left[\int_0^\infty G_1^2(\omega)\, \Phi_{11}(\omega)\, d\omega\right]\left[\int_0^\infty G_2^2(\omega)\, \Phi_{22}(\omega)\, d\omega\right]\right\}^{1/2}}$$

There are two possible simplifications available at this point. If the input were of a harmonic nature, say at frequency ω, then the expressions for spectral density would simplify and yield:

$$\langle e_1^2 \rangle = \int_0^\infty \Phi_{11}(\omega)\,\delta(\omega-\omega_1)\,d\omega = \Phi_{11}(\omega_1)$$

$$\langle e_2^2 \rangle = \int_0^\infty \Phi_{22}(\omega)\,\delta(\omega-\omega_1)\,d\omega = \Phi_{22}(\omega_1)$$

$$\langle e_1 e_2 \rangle = \int_0^\infty \Phi_{12}(\omega)\,\delta(\omega-\omega_1)\,d\omega = \Phi_{12}(\omega_1) \qquad \text{(C7)}$$

similarly:

$$\langle \hat{e}_1^2 \rangle = \int_0^\infty \Phi_{11}(\omega)\,G_1^2(\omega)\,\delta(\omega-\omega_1)\,d\omega = \Phi_{11}(\omega_1)\,G_1^2(\omega)$$

$$\langle \hat{e}_2^2 \rangle = \int_0^\infty \Phi_{22}(\omega)\,G_2^2(\omega)\,\delta(\omega-\omega_1)\,d\omega = \Phi_{22}(\omega)\,G_2^2(\omega) \qquad \text{(C8)}$$

$$\langle \hat{e}_1 \hat{e}_2 \rangle = \int_0^\infty \Phi_{12}(\omega)\,G_1(\omega)\,G_2(\omega)\,\delta(\omega-\omega_1)\,d\omega = \Phi_{12}(\omega_1)\,G_1(\omega_1)\,G_2(\omega_1)$$

and the dependence of the zero time lag cross-correlation coefficient upon the system's transfer function would disappear due to cancellation.

However, if the input were of a random nature, then the only simplification readily available is to have:

$$G_1(\omega) = G_2(\omega) = 1.0$$

in which case the original input cross-correlation is obtained since the system transfer function factors out from the integrands, cancels, and simplifies to equations:

$$\langle \hat{e}_1^2 \rangle = \langle e_1^2 \rangle = \int_0^\infty \Phi_{11}(\omega)\,d\omega$$

$$\langle \hat{e}_2^2 \rangle = \langle e_2^2 \rangle = \int_0^\infty \Phi_{22}(\omega)\,d\omega \qquad \text{(C9)}$$

$$\langle \hat{e}_1 \hat{e}_2 \rangle = \langle e_1 e_2 \rangle = \int_0^\infty \Phi_{12}(\omega)\, d\omega$$

Thus:

$$R_{12}(0) = \hat{R}_{12}(0) \tag{C10}$$

Since the latter case also applies to the harmonic signal data processing, this is a most desirable situation and is the motivation behind seeking a flat frequency of 1.00 ± 0.05.

LIST OF REFERENCES

1. National Aero- and Astronautical Research Institute Report NLR-TR F. 238., Theoretical and Experimental Results for the Dynamic Response of Pressure Measuring Systems, by H. Bergh and H. Tijdeman, January 1965.

2. Johnson, R. B., A Technique for Measuring Unsteady Pressures, A.E. Thesis, Naval Postgraduate School, Monterey, California, September 1968.

3. Allen, T. J., Pressure Distribution on an Airfoil in an Oscillating Flow, M.S.A.E. Thesis, Naval Postgraduate School, Monterey, California, June 1969.

4. McLachlan, N. W., Bessel Functions for Engineers, 2d ed., Oxford University Press, 1961.

5. Olson, H. F., Dynamical Analogies, 2d ed., D. van Nostrand Co., Inc., 1958.

6. Schmidt, L. V., Measurement of Fluctuating Air Loads on a Circular Cylinder, Ph.D. Thesis, California Institute of Technology, 1963.

7. Jesberg, R. H., Data Handling System in Support of Antenna Vibration Project, M.S. Thesis, Naval Postgraduate School, Monterey, California, 1966.

8. Bendat, J. S., and Allan G. Piersol, Measurement and Analysis of Random Data, John Wiley & Sons, Inc., 1966.

INITIAL DISTRIBUTION LIST

		No. Copies
1.	Defense Documentation Center Cameron Station Alexandria, Virginia 22314	2
2.	Library, Code 0212 Naval Postgraduate School Monterey, California 93940	2
3.	Chairman, Department of Aeronautics Naval Postgraduate School Monterey, California 93940	1
4.	Professor Louis V. Schmidt Department of Aeronautics Naval Postgraduate School Monterey, California 93940	1
5.	Lt(jg) John M. Lewis II 2341 General Bradley, N.E. Albuquerque, New Mexico 87112	1

DOCUMENT CONTROL DATA - R & D

(Security classification of title, body of abstract and indexing annotation must be entered when the overall report is classified)

1. ORIGINATING ACTIVITY (Corporate author)
Naval Postgraduate School
Monterey, California 93940

2a. REPORT SECURITY CLASSIFICATION

2b. GROUP

3. REPORT TITLE
Development of a Flat Frequency Response Pressure Transducer System

4. DESCRIPTIVE NOTES (Type of report and, inclusive dates)
Master's Thesis; June 1970

5. AUTHOR(S) (First name, middle initial, last name)
John M. Lewis, II

6. REPORT DATE
June 1970

7a. TOTAL NO. OF PAGES
56

7b. NO. OF REFS
8

8a. CONTRACT OR GRANT NO.

b. PROJECT NO.

c.

d.

9a. ORIGINATOR'S REPORT NUMBER(S)

9b. OTHER REPORT NO(S) (Any other numbers that may be assigned this report)

10. DISTRIBUTION STATEMENT
This document has been approved for public release and sale; its distribution is unlimited.

11. SUPPLEMENTARY NOTES

12. SPONSORING MILITARY ACTIVITY
Naval Postgraduate School
Monterey, California 93940

13. ABSTRACT

A theoretical prediction to determine the frequency response of a cascaded remote pressure transducer system has been developed. This prediction was used to find a theoretical configuration which would produce a fairly flat frequency response (1.00 ± 0.05) over a 100 hertz range. Such a configuration would allow cross-correlation of an unsteady, random, low-speed flow field by simple analog methods.

The theoretical prediction did not hold true for configurations of three serially connected tubes, but the parameters, namely, transducer volume, tube length, and tube diameter, proved the same trends experimentally that were predicted theoretically. By observing these trends, a solution of 1.00 ± 0.09 over a 95 hertz range was obtained.

14 KEY WORDS	LINK A		LINK B		LINK C	
	ROLE	WT	ROLE	WT	ROLE	WT
Pressures transducers Cross-correlation coefficient Oscillating flow						

Thesis 122450
L612 Lewis
c.1 Development of a
flat frequency re-
sponse pressure trans-
ducer system.
13 APR 72 9579
20 OCT 72 20938

Thesis 122450
L612 Lewis
c.1 Development of a
flat frequency re-
sponse pressure trans-
ducer system.

thesL612
Development of a flat frequency response
3 2768 002 11886 1
DUDLEY KNOX LIBRARY